



LUND UNIVERSITY

Remote imaging laser-induced breakdown spectroscopy and remote cultural heritage ablative cleaning

Grönlund, Rasmus; Lundqvist, M; Svanberg, Sune

Published in:
Optics Letters

2005

[Link to publication](#)

Citation for published version (APA):

Grönlund, R., Lundqvist, M., & Svanberg, S. (2005). Remote imaging laser-induced breakdown spectroscopy and remote cultural heritage ablative cleaning. *Optics Letters*, 30(21), 2882-2884.
<http://www.opticsinfobase.org/abstract.cfm?URI=ol-30-21-2882>

Total number of authors:
3

General rights

Unless other specific re-use rights are stated the following general rights apply:

Copyright and moral rights for the publications made accessible in the public portal are retained by the authors and/or other copyright owners and it is a condition of accessing publications that users recognise and abide by the legal requirements associated with these rights.

- Users may download and print one copy of any publication from the public portal for the purpose of private study or research.
- You may not further distribute the material or use it for any profit-making activity or commercial gain
- You may freely distribute the URL identifying the publication in the public portal

Read more about Creative commons licenses: <https://creativecommons.org/licenses/>

Take down policy

If you believe that this document breaches copyright please contact us providing details, and we will remove access to the work immediately and investigate your claim.

LUND UNIVERSITY

PO Box 117
221 00 Lund
+46 46-222 00 00

Remote imaging laser-induced breakdown spectroscopy and remote cultural heritage ablative cleaning

Rasmus Grönlund, Mats Lundqvist, and Sune Svanberg

Atomic Physics Division, Lund Institute of Technology, P.O. Box 118, S-221 00 Lund, Sweden

Received July 11, 2005

We report, for what we believe to be the first time, on remote imaging laser-induced breakdown spectroscopy (LIBS). Measurements have been performed by using a tripled Nd:YAG laser working at 355 nm with 170 mJ pulse energy, with an expanded beam that is focused onto a target at 60 m distance. The LIBS signal is detected by using an on-axis Newtonian telescope and an optical multichannel analyzer. The imaging is performed by scanning the laser beam on the target. The same setup is also used in demonstrations of remote laser ablation for cleaning of contaminated objects with applications toward cultural heritage.

© 2005 Optical Society of America

OCIS codes: 280.3640, 300.6360, 240.6490.

Laser-induced breakdown spectroscopy (LIBS) is a powerful method for material elemental analysis based on emission spectroscopy.^{1,2} It has been widely applied in analytical chemistry.³ LIBS can be applied remotely, as demonstrated in early Russian work^{4,5} and more recently by Palanco *et al.*,⁶ Rohwetter *et al.*,⁷ and our group.⁸ Lidar techniques were employed using CO₂, Nd:YAG, and short-pulse femtosecond laser systems. Remote detection from selected spots has been demonstrated, but imaging has not been performed previously. In a parallel development, remote LIBS is now being developed for deployment on remotely operated Mars landing vehicles.⁹

Laser ablation, where laser pulses are employed for explosive evaporation of small amounts of surface materials, is a technique widely used for micromachining and thin-film fabrication. It is also used for surface cleaning in the field of cultural heritage management, e.g., of paintings or statues,¹⁰ over short ranges.

Remote-imaging LIBS and remote ablative cleaning of stone surfaces are described in the present Letter, we believe for the first time. The Lund mobile lidar system, which was recently thoroughly upgraded,¹¹ was used in the present work. The experiments were performed with a system–target distance of 60 m. The important aspects of the lidar system regarding the present work on LIBS and remote ablation are noted in Fig. 1. We use frequency-tripled radiation (355 nm) from a 20 Hz pulsed Nd:YAG laser, and the radiation is transmitted toward the target via a 10 cm diameter specially designed refractive transmission telescope placed coaxially with the receiving 40 cm diameter reflective Newtonian telescope. The transmission and receiving beam paths are folded via a roof-top 40 × 80 cm first-surface aluminized mirror, which is controlled by stepper motors for precision scanning of the target.

A key aspect of remote LIBS and remote surface ablation is to ensure that a sufficiently high optical field strength can be achieved in the remote focus to induce a plasma breakdown at the solid target

surface. Clearly, because of diffraction, the laser beam must first be expanded and transmitted through a low-aberration telescope, which was designed with the aid of a ray-tracing program (Linos Photonics, WinLens 4.3). One plano-concave and two plano-convex lenses with focal lengths of, −25, 500, and 1000 mm and spaced by ~20 and ~25 cm were employed. The beam diameter and the laser pulse energy chosen must be matched in such a way that a laser spark is induced at the target without causing optical damage in the transmission system, especially damage of the aluminized folding mirror. We normally employed 170 mJ, 4–5 ns long pulses at 355 nm, generated by a Spectra-Physics Model GCR-290 Nd:YAG laser. While a focal-spot diameter of about 0.7 mm at a 60 m distant target is calculated, in practice we noted burn marks with a diameter of about 5 mm. The selection of tripled Nd:YAG radiation instead of doubled (532 nm) or fundamental (1064 nm) radiation is governed by eye-safety considerations (outside the focus, the UV beam reaches eye-safe intensity levels comparatively fast). Further, the

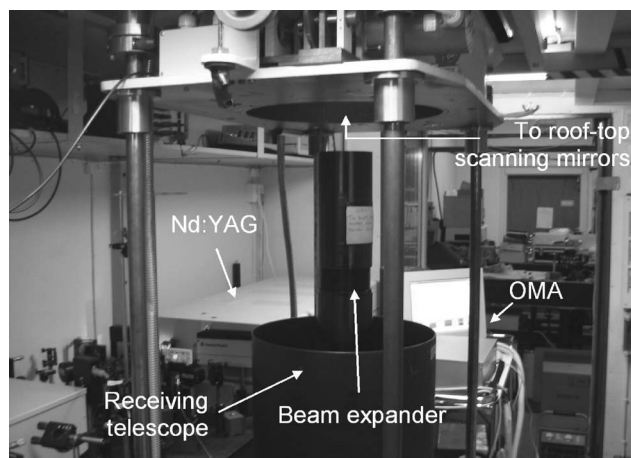


Fig. 1. Measurement setup with the important parts of the interior of the lidar system labeled. Detailed diagrams of the optical and electronic arrangements of the lidar system can be found in Ref. 11.

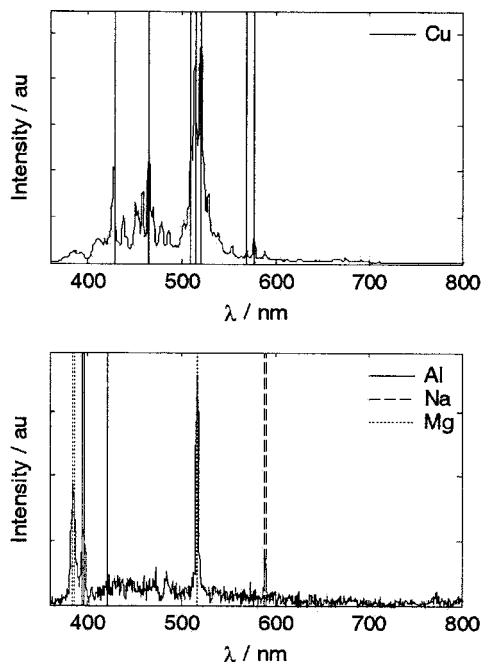


Fig. 2. Remote LIBS spectra from metal plates of copper and aluminum. The vertical lines correspond to tabular values of prominent emission peaks.¹² Note that magnesium and sodium contamination can be clearly seen in the aluminum case.

use of UV radiation allows plasma light to be detected throughout the visible region, and fluorescence can also be efficiently induced.

The plasma light collected by the lidar receiving telescope is focused into a 600 μm diameter optical fiber, which is connected to the entrance slit of an Oriel Corporation MS125 400 lines mm^{-1} grating spectrometer equipped with an Andor DH50125U-01 gated and intensified ccd detector. The 360–800 nm spectral region is detected with a spectral resolution of 2.2 nm. The intensifier is activated with a temporal window typically of 150 ns, which can be temporally located to match the arrival of the prompt target emission or delayed to allow observation of the plasma afterglow.

The present measurements were performed in Lund with the lidar system parked at the Physics Department, with the target area located on an easily accessible roof and with a brick wall terminating any stray laser pulses. Laser pulses are transmitted from the lidar roof-top mirror 4 m above the ground level in a completely safe manner. The lidar system is equipped with two TV cameras surveying the target area through the roof-top transmission dome, with clear marking of the exact target spot. As targets, arrangements of metal plates made of different elements were used. In addition, stone samples and even statues were utilized.

As an example of remote LIBS spectra, in Fig. 2 we show emission lines from copper and aluminum targets, recorded 300 ns after ablation with a 150 ns gate. The vertical lines correspond to tabular values of prominent emission lines of different elements.¹² Note that magnesium and sodium contamination can be seen in the case of aluminum.

By scanning the laser beam under computer control, it was possible to generate LIBS images such as shown in Fig. 3. A photograph of the target is included. By image processing, looking at the characteristic lines of different elements, it was possible to identify the target materials as shown in the figure.

The energy deposited in the plasma is sufficient to perform ablation and surface layer removal. On metal targets clear ablation marks could be seen. Oxide layers could be removed; even the green copper hydroxide typical of copper roofs at coastline locations could be ablated, and spectral differences could be noted as the surface was cleaned. Surface layer removal from stone surfaces has considerable value in terms of cultural heritage management. Thus, biodegradation layers on weathered mortar surfaces could be removed as well as corresponding coatings on granite rock [Fig. 4(a)]. Pencil and marker-pen blackened areas on white alabaster slabs (Volterra, Italy) could be readily removed [Fig. 4(b)] at a working speed of about $10 \text{ cm}^2 \text{ min}^{-1}$. Ablation speeds were similar for all the substances. The ablation process is basically self-terminating when the white substrate is reached. Here the samples were manually moved in a fixed beam. For a realistic remote cleaning of a statue, a 1 m tall white Italian garden replica statue partially covered by dirt and algal growth after ten years of weather exposure was used as a target. The remote cleaning of the statue with computerized beam scanning is illustrated in Fig. 4(c). Finally, an Italian replica statue head, made of white Carrara marble, was exposed, and an area heavily blackened by a soft pencil was cleaned [Fig. 4(d)]. No detectable surface damage could be observed by the naked eye.

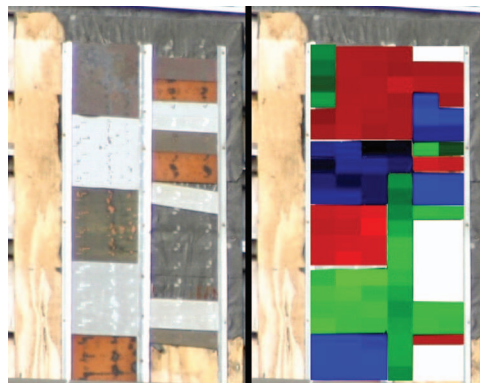


Fig. 3. LIBS imaging of metal plates, with the target on the left and a false-color coded identification image on the right with copper (red), aluminum (green) and iron (blue). The classification has good correspondence to the spots where the laser has hit the target. The big plates on the left are (from top to bottom) copper, stainless steel, brass, aluminum, and iron. The stainless steel is classified as iron and the brass as copper, as they contain large amounts of these substances. The vertical profiles holding the plates are made of aluminum and are classified accordingly. Note that the pixels are much larger than the spot size and that the scanning resolution is quite low. The beam scanning has been slightly tilted, and the middle spot in the upper rows does not hit the aluminum profile but instead hits the metal plates. White parts correspond to nonmetallic surfaces.

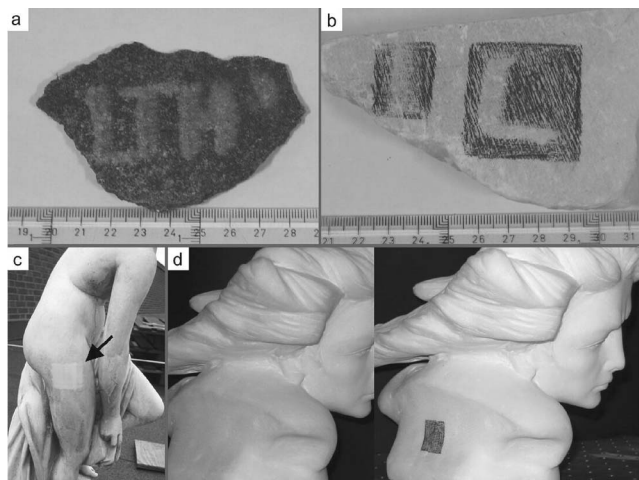


Fig. 4. Remote laser ablative cleaning of, a, mortar; b, alabaster; c, a replica of an Italian statue with the arrow indicating the 100 cm² cleaned area; d, a statue made of Carrara marble after and before cleaning.

Fluorescence and line emission spectra could be expected to change as the ablation of the surface layer proceeds and the substrate is reached. Thus the spectroscopic signals might be used to control the ablation in a similar way as coronary artery ablation can be supervised by a spectroscopic signal recorded through the fiber used as discussed, e.g., in Ref. 13.

It should be noted that the experiment described could, as in earlier laser-induced fluorescence lidar campaigns,^{14,15} have been performed at any historical monument, since the mobile lidar system is fully self-contained and is equipped with a 40 kVA motor generator towed by the lidar truck.

The present work shows that remote imaging LIBS can be used for surface assessment at considerable standoff distance and thus constitutes a complement to remote fluorescence imaging, e.g., in the assessment of historical monuments. Further, remote laser ablation with spectroscopic guidance seems to be a realistic possibility, which could reduce the cost of very expensive scaffolding in restoration work. Clearly, only areas directly seen from the ablation lidar system can be cleaned; however, on the other hand, these are the only ones that are visible to the spectator.

This work was supported by the Swedish Research Council for Environment, Agricultural Sciences and Spatial Planning (FORMAS) and by the Knut and Alice Wallenberg Foundation. Valuable assistance from Gabriel Somesfalean, Magnus Bengtsson, and Hans Edner in the early stage of the experiment is gratefully acknowledged.

References

1. L. J. Radziemski, T. R. Loree, D. A. Cremers, and N. M. Hoffman, *Anal. Chem.* **55**, 1246 (1983).
2. D. A. Cremers and L. J. Radziemski, in *Laser Spectroscopy and its Applications*, L. J. Radziemski, R. W. Solarz, and J. A. Paisner, eds. (Dekker, 1989), p. 351.
3. Special issue on LIBS, *Spectrochim. Acta, Part B* **56**, 565 (2002).
4. Iu. V. Akhtyrchenko, E. B. Beliaev, Iu. P. Vysotskii, O. V. Garin, A. P. Godlevskii, V. E. Zuev, Iu. D. Kopytin, A. I. Kuriapin, V. A. Pogodaev, and V. V. Pokasov, *Fizika (Alma Ata)* **26**, 5 (1983).
5. V. E. Zuev, Y. D. Kopytin, V. A. Korolkov, M. E. Levitskii, M. F. Nebolsin, B. G. Sidorov, and N. P. Soldatkin, in *Proceedings of the 13th International Laser Radar Conference* (NASA Langley Research Center, 1986).
6. S. Palanco, J. M. Baena, and J. J. Laserna, *Spectrochim. Acta, Part B* **57**, 591 (2002).
7. Ph. Rohwetter, J. Yu, G. Méjean, K. Stelmazczyk, E. Salmon, J. Kasparian, J. P. Wolf, and L. Wöste, *J. Anal. At. Spectrom.* **19**, 437 (2004).
8. R. Grönlund, M. Bengtsson, M. Sjöholm, G. Somesfalean, T. Johansson, P. Weibring, H. Edner, S. Svanberg, J. Hällström, and K. Barup, in *Air Pollution and Cultural Heritage*, C. Saiz-Jimenez, ed. (A. A. Balkema, 2004).
9. R. C. Wiens, S. Maurice, D. A. Cremers, and S. Chevrel, *Lunar Planet. Sci.* **34**, 1646 (2003).
10. C. Fotakis, S. Georgiou, V. Zafiropoulos, and V. Tornari, in *Proc. SPIE* **4402**, 8 (2001).
11. P. Weibring, H. Edner, and S. Svanberg, *Appl. Opt.* **42**, 3583 (2003).
12. D. R. Lide, ed., *CRC Handbook of Chemistry and Physics*, 74th ed. (CRC Press, 1993).
13. S. Svanberg, *Phys. Scr.* **T72**, 69 (1997).
14. P. Weibring, Th. Johansson, H. Edner, S. Svanberg, B. Sundnér, V. Raimondi, G. Cecchi, and L. Pantani, *Appl. Opt.* **40**, 6111 (2001).
15. D. Lognoli, G. Cecchi, I. Mochi, L. Pantani, V. Raimondi, R. Chiari, Th. Johansson, P. Weibring, H. Edner, and S. Svanberg, *Appl. Phys. B* **76**, 457 (2003).